

Article

Ensemble Negatively-Charged Nitrogen-Vacancy Centers in Type-Ib Diamond Created by High Fluence Electron Beam Irradiation

Shuya Ishii^{1,2,*}, Seiichi Saiki^{1,*}, Shinobu Onoda^{1,2}, Yuta Masuyama¹, Hiroshi Abe^{1,2}
and Takeshi Ohshima^{1,2}

- ¹ Takasaki Advanced Radiation Research Institute, National Institutes for Quantum Science and Technology, 1233 Watanuki, Takasaki 370-1292, Japan; onoda.shinobu@qst.go.jp (S.O.); masuyama.yuta@qst.go.jp (Y.M.); abe.hiroshi2@qst.go.jp (H.A.); ohshima.takeshi@qst.go.jp (T.O.)
- ² Institute for Quantum Life Science, National Institutes for Quantum Science and Technology, 4-9-1 Anagawa, Inage-ku, Chiba 263-8555, Japan
- * Correspondence: ishii.shuya@qst.go.jp (S.I.); saiki.seiichi@qst.go.jp (S.S.)
- † These authors contributed equally to this work.

Abstract: Electron beam irradiation into type-Ib diamond is known as a good method for the creation of high concentration negatively-charged nitrogen-vacancy (NV⁻) centers by which highly sensitive quantum sensors can be fabricated. In order to understand the creation mechanism of NV⁻ centers, we study the behavior of substitutional isolated nitrogen (P1 centers) and NV⁻ centers in type-Ib diamond, with an initial P1 concentration of 40–80 ppm by electron beam irradiation up to 8.0×10^{18} electrons/cm². P1 concentration and NV⁻ concentration were measured using electron spin resonance and photoluminescence measurements. P1 center count decreases with increasing irradiation fluence up to 8.0×10^{18} electrons/cm². The rate of decrease in P1 is slightly lower at irradiation fluence above 4.0×10^{18} electrons/cm² especially for samples of low initial P1 concentration. Comparing concentration of P1 centers with that of NV⁻ centers, it suggests that a part of P1 centers plays a role in the formation of other defects. The usefulness of electron beam irradiation to type-Ib diamonds was confirmed by the resultant conversion efficiency from P1 to NV⁻ center around 12–19%.

Keywords: electron irradiation; type-Ib diamond; NV center; quantum sensor



Citation: Ishii, S.; Saiki, S.; Onoda, S.; Masuyama, Y.; Abe, H.; Ohshima, T. Ensemble Negatively-Charged Nitrogen-Vacancy Centers in Type-Ib Diamond Created by High Fluence Electron Beam Irradiation. *Quantum Beam Sci.* **2022**, *6*, 2. <https://doi.org/10.3390/qbs6010002>

Academic Editor: Swee Leong Sing

Received: 19 November 2021

Accepted: 28 December 2021

Published: 30 December 2021

Publisher's Note: MDPI stays neutral with regard to jurisdictional claims in published maps and institutional affiliations.



Copyright: © 2021 by the authors. Licensee MDPI, Basel, Switzerland. This article is an open access article distributed under the terms and conditions of the Creative Commons Attribution (CC BY) license (<https://creativecommons.org/licenses/by/4.0/>).

1. Introduction

The negatively-charged nitrogen-vacancy (NV⁻) center in diamond is a lattice defect consisting of one nitrogen atom adjacent to one atomic vacancy (Figure 1) [1,2]. The NV⁻ center has been in the center of attention as a qubit for quantum information processing, and also as a quantum sensor for detection of magnetic field, electric field, temperature and strain, etc. [3]. The multifunctional property of NV⁻ centers working at room temperature (RT) is very attractive for many research fields; especially in the field of biology and life sciences [4–7]. Quantum beam irradiation followed by subsequent thermal annealing is one of the effective procedures to create NV⁻ center in diamond [8]. The irradiation introduces vacancies into diamond containing nitrogen atoms, and the annealing enables vacancies to diffuse. Then diffused vacancies are trapped by nitrogen atoms, and as a result, NV centers are formed. In addition, by one electron supplied from another nitrogen atom at a lattice site (P1 center), the charge state of NV centers changes from neutral (NV⁰) to NV⁻.

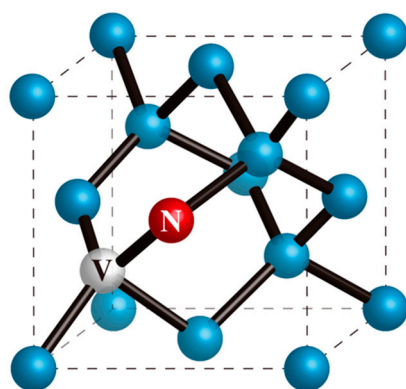


Figure 1. A schematic illustration of a NV center in diamond lattice consists of a substitutional nitrogen atom (red), an atomic vacancy (white) and carbon atoms (blue).

Applying NV^- centers in quantum sensing requires high concentration of ensemble NV^- centers to achieve high sensitivities [3,5]. For example, the magnetic sensitivity is proportional to the reciprocal of $\sqrt{NT_2}$, where N is the number of NV centers and T_2 is the spin coherence time. The dense NV^- centers with long T_2 increase the sensitivity. For this purpose, MeV-range electron beam irradiation into a type-Ib diamond is a promising methodology, since a type-Ib diamond contains high concentration of P1 centers, and an electron beam enables creation of atomic vacancies uniformly both in-plane and in-depth, up to several mm deep [9]. The high-concentration NV^- centers have been studied and developed for quantum sensor application [10–13]. It is known that P1 center has an important role for not only being a component of NV^- centers, but also by supplying a negative charge to the NV center. However, there is still room to understand the mechanism of NV creation in diamond with high concentrations of P1 centers. If the concentration of P1 centers, which act as electron donors, is lower than certain concentration, the charge state of NV centers becomes neutral [14,15]. The neutral NV (NV^0) centers do not act as quantum sensor and deteriorate sensitivity of sensor due to lower signal contrast of optically detected magnetic resonance (ODMR). P1 centers play a role not only for NV^- center creation, but also as decoherence source (decrease in magnetic field sensitivity) [3]. Therefore, it is important to create high concentration of NV^- centers without NV^0 , considering the amount of P1 centers.

In this study, we investigate irradiation fluence dependence of the creation behavior of NV centers in type-Ib diamonds by using electron spin resonance (ESR) and photoluminescence (PL) to understand the creation mechanism of NV^- center. Moreover, the values of T_2 are evaluated by Hahn-echo sequencing, since the value is one of the key parameters for highly sensitive AC magnetometry [3,16]. Then, we discuss the creation mechanism of NV centers based on decreasing P1 and increasing NV concentrations due to electron beam irradiation.

2. Materials and Methods

Commercially available type-Ib diamonds synthesized by high-pressure-high-temperature (HPHT) method (Sumitomo Electric Industries, Osaka, Japan) were used in this study. The initial P1 concentrations ($[P1]_{\text{initial}}$) for the samples were measured by ESR and referred to as Ib-80, Ib-72, Ib-52, Ib-46 depending on $[P1]_{\text{initial}}$ of 80, 72, 52, and 46 ppm, respectively. Before electron beam irradiation, diamond samples were treated with the mixture of sulfuric acid and nitric acid around 200 °C to remove surface contamination. Electron beam irradiation in atmosphere at an energy of 2 MeV was carried out with irradiation fluence up to 8.0×10^{18} electrons (e)/cm² (total irradiation time; 80 h, Fluence rate; 1.0×10^{17} e/cm²/h) at Takasaki Advanced Radiation Research Institute, QST, Japan. The samples were kept on a water-cooled copper plate to avoid heating up of sample during irradiation. Subsequently, irradiated samples were annealed in furnace at 1000 °C for 2 h in vacuum ($\sim 1.0 \times 10^{-4}$ Pa) at each fluence step.

ESR spectra were obtained with an X-band spectrometer (JES-X330, JEOL Ltd., Tokyo, Japan) at RT. Concentrations of P1 center ([P1]) and NV⁻ center ([NV⁻]) in diamond were determined by comparing their double-integrated ESR intensity to that of a reference sample, which is a HPHT synthetic type-Ib diamond containing 34 ± 3 ppm of P1 centers.

PL spectra were acquired with spectrometer (LabRAM HR Evolution, HORIBA, Kyoto, Japan) at RT. The excitation laser ($\lambda = 532$ nm) was led through the objective lens (MPlan N, 100X, N.A. = 0.9, Olympus) and the laser power was fixed at low value (800 nW) to prevent transition from NV⁻ to NV⁰ [10]. The ratio between NV⁰ and NV⁻ was obtained by fitting the typical spectra of NV⁰ and NV⁻ spectrum to each spectrum data. Afterwards, the ratio was corrected with the difference in fluorescence lifetime (NV⁰, NV⁻) [17,18].

The values of T_2 of NV⁻ center ensembles were measured using a home-built fluorescent microscope with a microwave system. The diamond sample was placed on a microwave resonator and excited by 532 nm laser (gem532, Laser Quantum, Stockport, UK). The fluorescence was detected using a photodiode (APD410A/M, Thorlabs, Newton, NJ, USA) and recorded via oscilloscope (MDO34, Tektronix, Beaverton, OR, USA). A magnetic field was applied to the sample by a permanent magnet, and the resonance frequency was identified by ODMR. Rabi oscillations of the ensemble NV center were measured to determine the state flip (π pulse) time, and a Hahn-echo sequence was performed to measure T_2 .

3. Results

3.1. Irradiation Fluence Dependence of P1 Center Concentration

By electron beam irradiation and subsequent annealing for type-Ib diamonds, some amounts of P1 centers are consumed through NV⁻ center creation. The consumption of P1 centers was evaluated by measuring [P1]. P1 centers can be detected by ESR, since a P1 center has an unpaired electron, $S = 1/2$. The ESR spectrum shows signal peaks at around approximately $g = 2$ split by hyperfine interaction with nitrogen nuclear spins, $I = 1$ (¹⁴N). The details of P1 center spectrum have been well established [19,20]. In this study, the center peaks are used for quantification of [P1]. Figure 2a shows center peaks of P1 centers for Ib-46 at irradiation fluence of 0.0, 3.5, 6.0, and 8.0×10^{18} e/cm². Obviously, the intensity decreases with increasing irradiation fluence. Figure 2b represents [P1] of four samples as a function of electron fluence. The uncertainty of [P1] is about $\pm 10\%$. For all samples, [P1] decreases with increasing irradiation fluence. However, P1 centers still remain in all samples even after irradiation with fluences up to 8.0×10^{18} e/cm². The residual P1 centers are expected to be converted to NV center by further irradiation. The relationship between the consumption of P1 and the creation NV⁻ will be discussed in Section 4.

3.2. Irradiation Fluence Dependence of NV⁻ Center Concentration

NV centers can be excited by green laser light (532 nm), and PL spectra were obtained to analyze the charge state and the amount of NV centers. NV⁰ and NV⁻ centers show zero-phonon lines (ZPLs) at 575 nm and 638 nm, respectively (Arrows in Figure 3a) [12]. In addition, each center has broad phonon-side-band at RT as shown in Figure 3a. The shown spectrum of NV⁰ in Figure 3a was typical one obtained from a CVD diamond sample containing a low density of [P1]_{initial}, irradiated with sufficient high fluence of electron beam. Thus, most P1 centers have been converted to NV centers and there is no P1 center acting as donor. At the measurement, a high power laser (8 mW) was used for excitation to induce transition from NV⁻ centers to NV⁰ centers [21]. On the other hand, the spectrum of Ib-80 with the irradiation fluence of 8.0×10^{18} e/cm², where the ZPL of NV⁰ center is absent, was regarded as typical spectrum of NV⁻ center (Figure 3a). All PL spectra obtained in this study were analyzed by fitting with superposition of typical spectra of NV⁻ and NV⁰ centers. Figure 3b represents PL spectra of four samples with the irradiation fluence of 8.0×10^{18} e/cm². No significant difference among all spectra is obtained although very small amount of ZPL for NV⁰ is observed for Ib-52. The NV⁻/NV⁰ ratio for Ib-52 is estimated to be around 175 or less. The obtained result indicates that most

NV centers created in all samples are NV^- , even after electron irradiation at the fluence of $8.0 \times 10^{18} \text{ e/cm}^2$, although very small amounts of NV^0 are created in Ib-52.

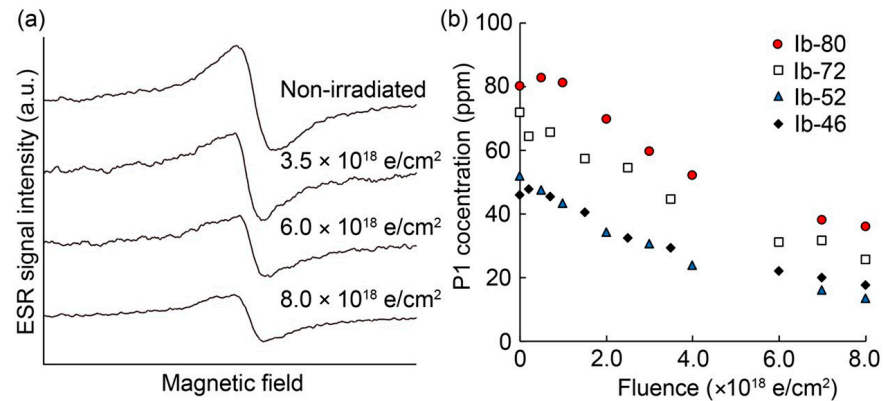


Figure 2. Irradiation fluence dependence of P1 center concentrations ([P1]) in type-Ib diamonds after irradiation and subsequent annealing. (a) ESR spectra of P1 center for Ib-46 at the irradiation fluence of 0.0, 3.5, 6.0, $8.0 \times 10^{18} \text{ e/cm}^2$. ([100]/ B_0) (b) Irradiation fluence dependence of [P1] for Ib-80 (closed red circles), Ib-72 (open black circles), Ib-52 (closed blue circles), Ib-46 (closed black circles), respectively.

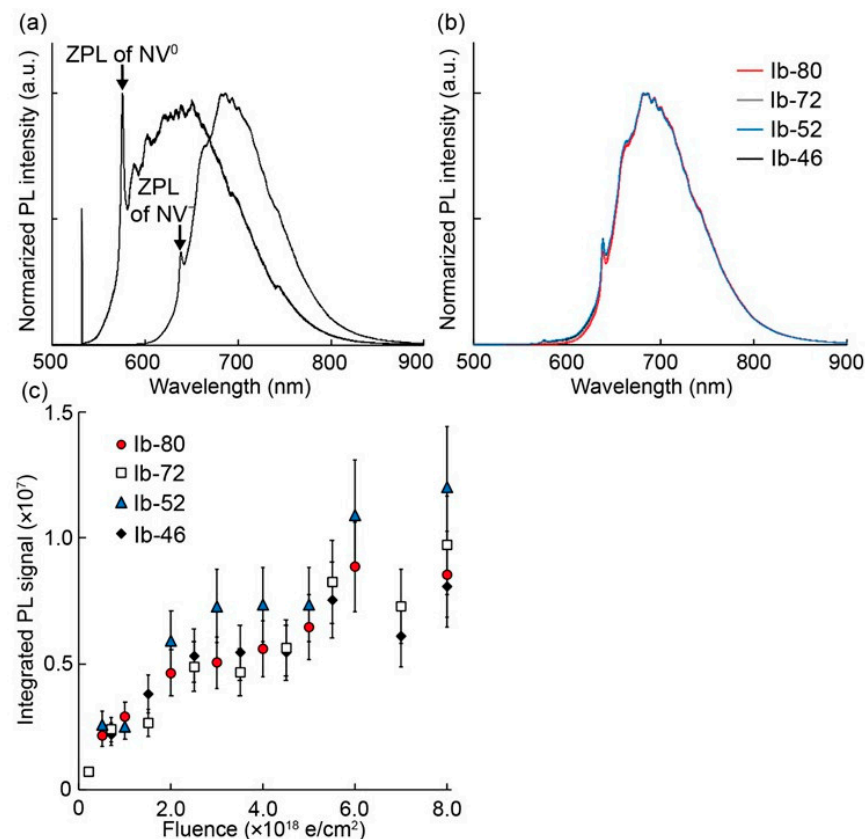


Figure 3. PL measurement of NV^- center in type-Ib diamonds after irradiation and subsequent annealing. (a) Typical PL spectra of NV^- and NV^0 center normalized by peak intensity. The typical spectra of NV^- and NV^0 center are obtained from Ib-80 and sample contains low P1 center concentration (~ 40 ppb), respectively. The peak at 532 nm is reflected excitation light. The spectra are normalized by peak intensity. (b) PL spectra at irradiation fluence of $8.0 \times 10^{18} \text{ e/cm}^2$ for Ib-80 (red line), Ib-72 (gray line), Ib-52 (blue line), Ib-46 (black line), respectively. These spectra are normalized by peak intensity. (c) Irradiation fluence dependence of integrated PL intensity for Ib-80 (closed red circles), Ib-72 (open black circles), Ib-52 (closed blue circles), Ib-46 (closed black circle), respectively.

Integrated values of PL spectra between 535 and 900 nm are plotted as a function of irradiation fluence in Figure 3c. The integrated signals for all samples increase with increasing irradiation fluences. This suggests that the amounts of NV^- center increase with increasing the irradiation fluence. To estimate the $[NV^-]$, we carried out an ESR study.

NV^- centers in triplet ground state can be observed by ESR [13,22]. The typical ESR spectrum of NV^- center shows eight peaks caused by zero-field-splitting by spin-spin interaction at ground triplet state and four orientations of its electron orbitals due to tetrahedral symmetry. Figure 4a represents the leftmost peak of NV^- centers where one crystallographic axes, $[111]$, is aligned to the external magnetic field (B_0). The spectra clearly show hyperfine splitting by nitrogen nuclear spins. The intensity of spectra obviously increases with increasing irradiation fluence. $[NV^-]$ was calculated and plotted as a function of irradiation fluence in Figure 4b. In contrast to P1 centers, NV^- centers increase with increasing irradiation fluence. As a result, 10 ppm of NV^- are created in Ib-80 by electron irradiation at the fluence of $8.0 \times 10^{18} \text{ e/cm}^2$.

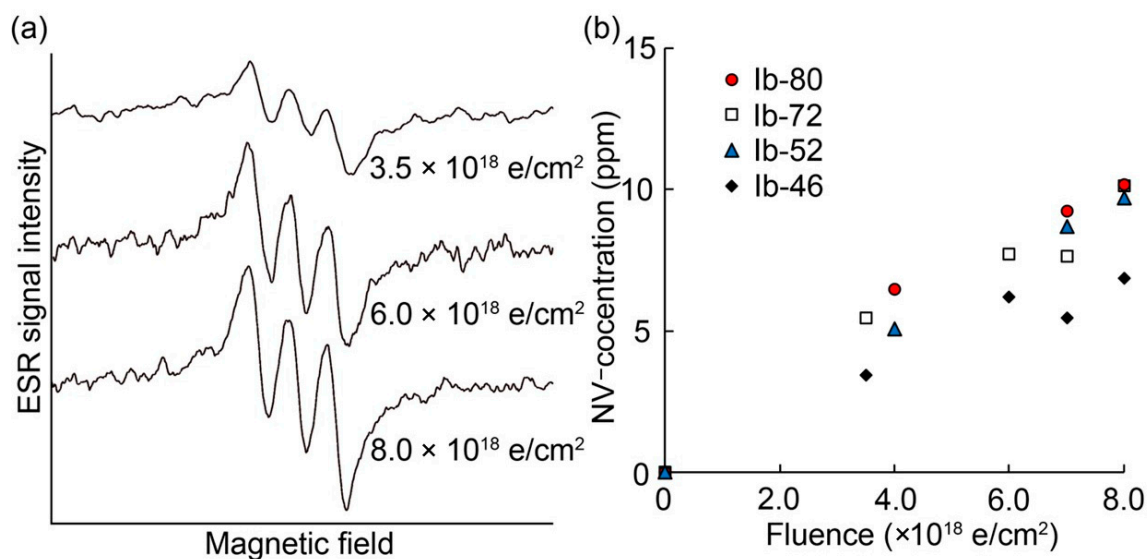


Figure 4. ESR measurement of NV^- center in type-Ib diamonds after irradiation and subsequent annealing. (a) Typical ESR spectra of a left most peak of NV^- center at the different irradiation fluence for Ib-46. ($[111]/B_0$) (b) Irradiation fluence dependence of NV^- center concentration ($[NV^-]$) for Ib-80 (closed red circles), Ib-72 (open black circles), Ib-52 (closed blue circles), Ib-46 (closed black circles), respectively.

3.3. Coherence Time (T_2) of Ensemble NV^- Center

Basically, longer T_2 and higher concentration of NV^- centers results in higher sensitivity for magnetometry [3,16]. Thus, T_2 plays a crucial role as one of indicators about the sensitivity of quantum sensing. In order to investigate spin relaxation property of samples irradiated at fluence of $8.0 \times 10^{18} \text{ e/cm}^2$, T_2 of NV^- centers was measured using Hahn-echo pulse sequences. The ODMR spectrum for Ib-72 irradiated at $8.0 \times 10^{18} \text{ e/cm}^2$ is shown in Figure 5a as an example for a typical ODMR signal. The resonance dips are split fourfold by an external magnetic field. Since the two center dips are degenerate groups of different crystallographic axes of diamond lattice of $[\bar{1}\bar{1}\bar{1}]$, $[1\bar{1}\bar{1}]$, and $[\bar{1}\bar{1}1]$, resonant frequency of nondegenerate group from $[1\bar{1}\bar{1}]$ at around 2.8 GHz was used to observe Rabi oscillations of the ensemble NV^- centers (Figure 5b). Spin-echo decay with free precession time measured by Hahn-echo sequences is depicted in Figure 5c. The value of T_2 for each sample was estimated from the spin-echo decay. T_2 of irradiated samples were obtained as follows: $(1.3 \pm 0.48) \mu\text{s}$ for Ib-80, $(1.6 \pm 0.77) \mu\text{s}$ for Ib-72, $(2.7 \pm 0.96) \mu\text{s}$ for Ib-52, $(2.1 \pm 0.68) \mu\text{s}$ for Ib-46.

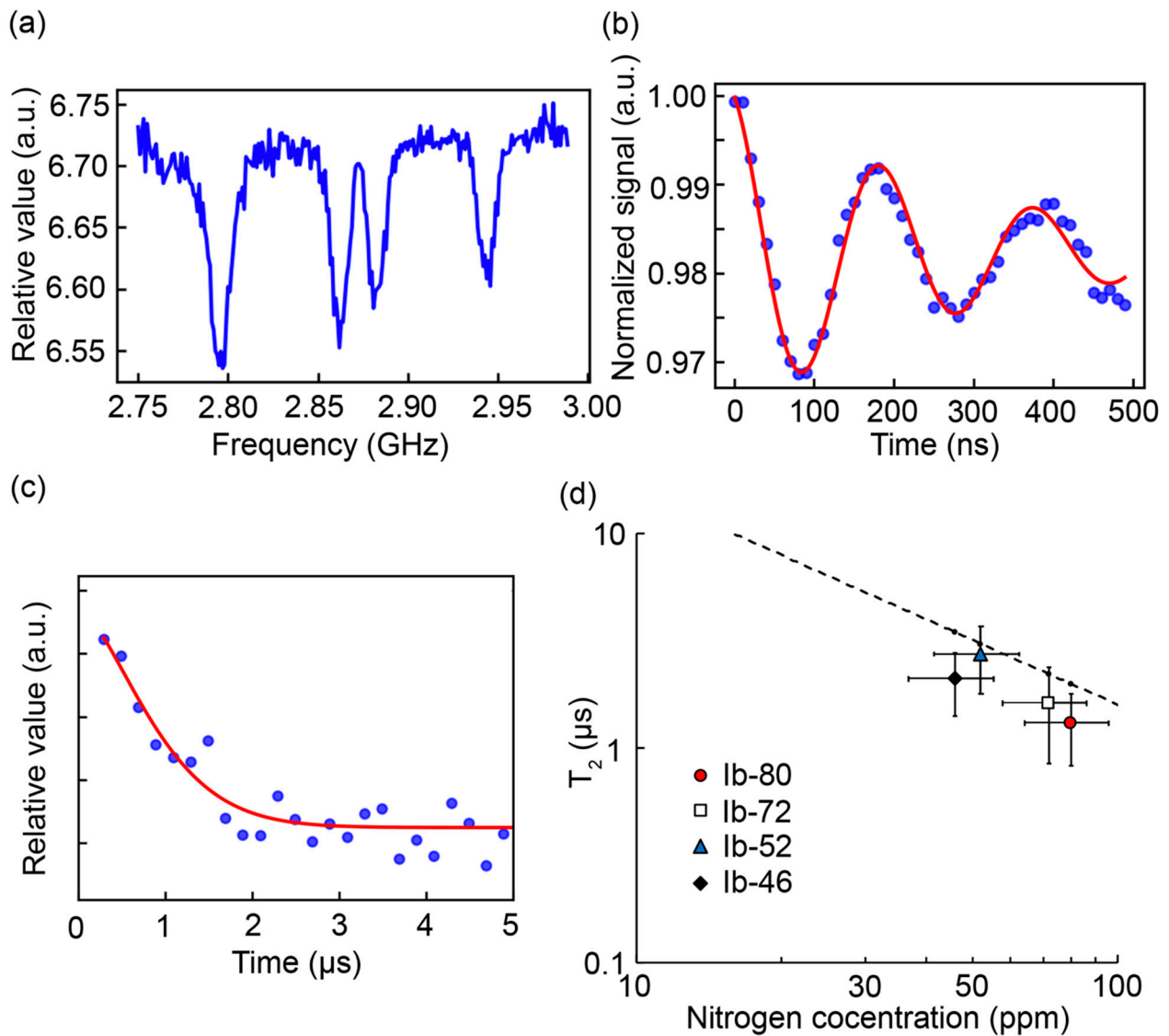


Figure 5. Evaluation of spin coherence time (T_2) of NV^- center in type-Ib diamond. (Sample: Ib-72 at fluence of $8 \times 10^{18} e/cm^2$ for (a–c)). (a) CW-ODMR spectra. (b) Rabi oscillation and fitting by damped sine curve. (c) Spin echo decay with free precession time and fitting by stretched exponential decay. (d) Dependence of nitrogen concentration on T_2 (Double logarithmic plot). Ib-80 (closed red circle), Ib-72 (open black circle), Ib-52 (closed blue circle), Ib-46 (closed black circle), respectively. Broken line shows Equation (1) [23].

According to Bauch et al. [23], T_2 depends on total nitrogen concentration when its value is more than 1 ppm, since the interaction with nitrogen spin bath is the dominant decoherence source for ensemble NV^- centers. Bauch et al. reported a following equation;

$$1/T_2([N_T]) = B_{NV-N} \cdot [N_T] + 1/T_{2,other} \quad (1)$$

where B_{NV-N} is the nitrogen-dominated NV^- decoherence rate per unit density; $T_{2,other}$ accounts for decoherence mechanisms independent of nitrogen and $[N_T]$ indicates total nitrogen concentration. The values of B_{NV-N} and $T_{2,other}$ were determined as $1/B_{NV-N} = (160 \pm 12) \mu s \text{ ppm}$ and $T_{2,other} = (694 \pm 12) \mu s$ in Ref. [23]. The values of T_2 obtained in this study are plotted as a function of nitrogen concentration in Figure 5d. In the calculation, we assume that the values of $[P1]_{initial}$ are equivalent to $[N_T]$. For comparison, the result obtained from the Equation (1) is also plotted as the dotted line in the figure. Obtained T_2 values in our experiment are compatible with the results estimated from Equation (1), and this means

that the T_2 obtained in this study is dominated by nitrogen concentration. Although, the results obtained from Ib-80, Ib-72, Ib-46 seem to be slightly below the line, and it suggests that further decoherence occurred by other defects.

4. Discussion

The main mechanism of NV^- center creation has been described by a simple model of two processes, as shown below [14].



where N_s^0 is the P1 center (neutral single-substitutional nitrogen), V^0 is the neutral vacancy produced by energetic particle irradiation, N_s^+ is the positively charged single-substitutional nitrogen which gives one electron to NV^0 center; resulting in NV^- being created. The first process (Equation (2)) represents combination of N_s^0 and V^0 by thermal annealing, resulting in NV^0 center creation. Thus, the vacancies diffuse in diamond during thermal annealing over 600 °C [24], and NV^0 centers are created when the vacancies reach P1 centers.

Here, Figure 2b was replotted in Figure 6a as the change in P1 center concentration from the $[P1]_{\text{initial}}$ ($\Delta[P1]$) due to electron irradiation followed by annealing. $\Delta[P1]$ for all samples decreases linearly with increasing irradiation fluence, especially for the low fluence range ($\sim 4.0 \times 10^{18} \text{ e/cm}^2$; see the broken line for visual guide). This result means that the consumption of P1 centers depends on irradiation fluence, but not on $[P1]_{\text{initial}}$ in the case of high $[P1]_{\text{initial}}$ density, such as 45–80 ppm. In other words, the creation of NV^- might be limited by the creation of vacancies. On the other hand, the decreasing rate of P1 center becomes lower with increasing irradiation fluence in fluence ranges from $6.0 \times 10^{18} \text{ e/cm}^2$ to $8.0 \times 10^{18} \text{ e/cm}^2$, and this tendency is larger when $[P1]_{\text{initial}}$ is smaller. Thus, the P1 center consumption is lower especially in low $[P1]_{\text{initial}}$ samples, although $[P1]$ still remains even after irradiation at fluence of $8.0 \times 10^{18} \text{ e/cm}^2$. This suggests that the probability of recombination of P1 centers and vacancies is lower due to smaller amounts of P1.

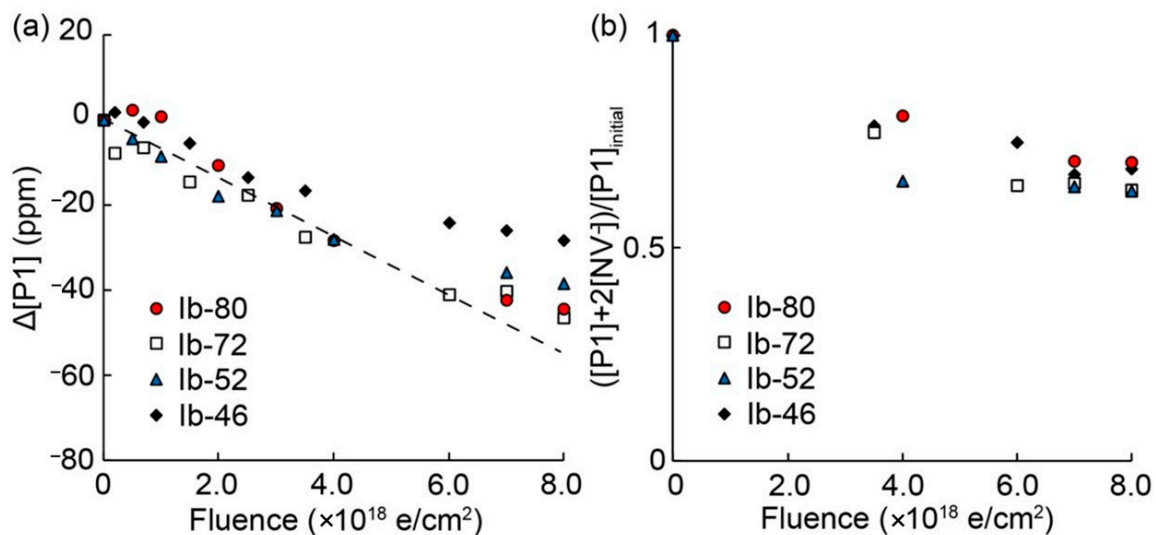


Figure 6. Conversion from P1 center to NV^- center. (a) Irradiation fluence dependence of $\Delta[P1]$ (changes from the $[P1]_{\text{initial}}$). Broken line is for visual guide. (b) Irradiation fluence dependence of value of $([P1] + 2[NV^-])/[P1]_{\text{initial}}$. Ib-80 (closed red circles), Ib-72 (open black circles), Ib-52 (closed blue circles), Ib-46 (closed black circles), respectively.

According to Equations (2) and (3), two P1 centers are consumed for the creation of one NV^- center ($2P1 \rightarrow NV^- + N_s^0$, one P1 for NV creation and another for electron donor). If this simple reaction can be applied to this result, the number of N_s^0 ($[N_s^0]$)

should be equal to the number of NV^- ($[NV^-]$). This means that $\Delta[P1]$ is equal to the twice $[NV^-]$ ($\Delta[P1] = 2[NV^-]$) because of $\Delta[P1] = [NV^-] + [N_s^0]$. Using an equation of $[P1]_{\text{initial}} = [P1] + \Delta[P1]$, the equation $[P1]_{\text{initial}} = [P1] + 2[NV^-]$ is derived. The values of $([P1] + 2[NV^-])/[P1]_{\text{initial}}$ for samples as a function of irradiation fluence are plotted in Figure 6b. If NV^- center creation can be explained in terms of the simple reaction describes as Equations (2) and (3), the value of $([P1] + 2[NV^-])/[P1]_{\text{initial}}$ should be unity. However, as shown in Figure 6b, the values of $([P1] + 2[NV^-])/[P1]_{\text{initial}}$ for all samples decrease with increasing electron fluence and become around 0.8 after irradiation at $8.0 \times 10^{18} \text{ e/cm}^2$. The values less than unity indicate that not all P1 centers are involved in the NV^- conversion. Thus, residual defects which contain nitrogen or/and capture charges are created due to the accumulation of irradiation damage. Since the creation yield of NV^- as well as the quality of NV^- (T_2) are affected by such residual defects (shown in Figure 5d), irradiation and annealing procedures must be improved. Further investigations are necessary to clarify this.

Conversion efficiency from nitrogen atom to NV^- center is a useful indicator to evaluate the NV^- center creation, which is defined as the ratio of $[NV^-]$ to $[N_T]$, where $[N_T]$ is the concentration of all nitrogen atoms [3]. Calculated conversion efficiencies of our samples at $8.0 \times 10^{18} \text{ e/cm}^2$ reached ~13% for Ib-80, ~14% for Ib-72, ~19% for Ib-52, ~15% for Ib-46, respectively, regarding $[P1]_{\text{initial}}$ as $[N_T]$. These values are consistent with previous studies [10], and are obviously higher than that of other procedures. For example, unmodified as-grown CVD process showed single-digit percentages [3,25]. Thus, the result obtained in this study suggests that electron beam irradiation into type-Ib diamond is useful to create NV^- centers with high concentration for quantum sensing.

5. Conclusions

We studied the creation behavior of NV center in type-Ib diamonds with high $[P1]_{\text{initial}}$ under relatively high irradiation fluences, by ESR and PL measurements, to understand the creation mechanism of NV^- centers. The decrease rate of P1 centers as a function of irradiation fluence shows similar tendencies for all type-Ib diamond samples, regardless of the initial P1 concentration ($[P1]_{\text{initial}}$; 40–80 ppm) in the low fluence range ($\sim 4.0 \times 10^{18} \text{ e/cm}^2$). The reduction rate of P1 centers suggests that P1 centers are consumed by recombination with introduced vacancies. However, the decrease rate of P1 became lower in the high fluence ranges from $6.0 \times 10^{18} \text{ e/cm}^2$ to $8.0 \times 10^{18} \text{ e/cm}^2$, especially when $[P1]_{\text{initial}}$ is smaller, in spite that [P1] still exists even after irradiation at $8.0 \times 10^{18} \text{ e/cm}^2$. The process of P1 center consumption seems to shift depending on the residual P1 centers. Furthermore, the P1 center consumption and NV^- center creation were compared and as a result, it is concluded that some amounts of the P1 centers were consumed by other defects. The conversion efficiency from $[P1]_{\text{initial}}$ to the $[NV^-]$ reached ~19% at $8.0 \times 10^{18} \text{ e/cm}^2$ and the value confirms the usefulness of electron beam irradiation for high concentration of NV^- centers in type-Ib diamonds, whereas results in this study suggest that not all P1 centers converted to NV^- center and the residual defects might lead to a cause of decoherence.

Author Contributions: Conceptualization, S.I., S.S., S.O. and T.O.; methodology, S.I., S.S., S.O., Y.M. and H.A.; software, S.O. and Y.M.; validation, S.I., S.S., S.O., Y.M. and T.O.; formal analysis, S.I., S.S. and S.O.; investigation, S.I., S.S. and S.O.; data curation, S.I., S.S. and S.O.; writing—original draft preparation, S.I., S.S., S.O. and T.O.; writing—review and editing, S.I., S.S., S.O., Y.M. and T.O.; visualization, S.I., S.S. and S.O.; supervision, S.O. and T.O.; project administration, S.O. and T.O.; funding acquisition, T.O. All authors have read and agreed to the published version of the manuscript.

Funding: This work was partially supported by Quantum Leap Flagship Program (Q-LEAP; JPMXS 0118067395) of MEXT.

Data Availability Statement: All data that shown in this manuscript are available from corresponding authors upon reasonable requests.

Acknowledgments: We thank Junichi Isoya at University of Tsukuba for valuable discussion on ESR analysis, Jan Jeske and Luo Tingpeng at Fraunhofer Institute for Applied Solid State Physics for valuable discussion on PL spectra analysis.

Conflicts of Interest: All authors declare no conflict of interest.

References

1. Abtew, T.A.; Sun, Y.Y.; Shih, B.; Dev, P.; Zhang, S.B.; Zhang, P. Dynamic Jahn-Teller effect in the NV⁻ center in diamond. *Phys. Rev. Lett.* **2011**, *107*, 146403. [[CrossRef](#)]
2. Dovesi, R.; Gentile, F.S.; Ferrari, A.M.; Pascale, F.; Salustro, S.; Arco, P.D.; Chimica, D.; Torino, U.; Giuria, V.P. On the models for the investigation of charged defects in solids: The case of the VN⁻ defect in diamond. *J. Phys. Chem. A* **2019**, *123*, 4806–4815. [[CrossRef](#)] [[PubMed](#)]
3. Barry, J.F.; Schloss, J.M.; Bauch, E.; Turner, M.J.; Hart, C.A.; Pham, L.M.; Walsworth, R.L. Sensitivity optimization for NV⁻ diamond magnetometry. *Rev. Mod. Phys.* **2020**, *92*, 015004. [[CrossRef](#)]
4. Hall, L.T.; Beart, G.C.G.; Thomas, E.A.; Simpson, D.A.; McGuinness, L.P.; Cole, J.H.; Manton, J.H.; Scholten, R.E.; Jelezko, F.; Wrachtrup, J.; et al. High spatial and temporal resolution wide-field imaging of neuron activity using quantum NV⁻ diamond. *Sci. Rep.* **2012**, *2*, 401. [[CrossRef](#)] [[PubMed](#)]
5. Kucsko, G.; Maurer, P.C.; Yao, N.Y.; Kubo, M.; Noh, H.J.; Lo, P.K.; Park, H.; Lukin, M.D. Nanometre-scale thermometry in a living cell. *Nature* **2013**, *500*, 54–58. [[CrossRef](#)]
6. Fujisaku, T.; Tanabe, R.; Onoda, S.; Kubota, R.; Segawa, T.F.; So, F.T.-K.; Ohshima, T.; Hamachi, I.; Shirakawa, M.; Igarashi, R. pH nanosensor using electronic spins in diamond. *ACS Nano* **2019**, *13*, 11726–11732. [[CrossRef](#)] [[PubMed](#)]
7. Igarashi, R.; Sugi, T.; Sotoma, S.; Genjo, T.; Kumiya, Y.; Walinda, E.; Ueno, H.; Ikeda, K.; Sumiya, H.; Tochio, H.; et al. Tracking the 3D rotational dynamics in nanoscopic biological systems. *J. Am. Chem. Soc.* **2020**, *142*, 7542–7554. [[CrossRef](#)]
8. Crookes, W. *Diamonds*; Harper & Brothers: London, UK; New York, NY, USA, 1909.
9. Campbell, B.; Mainwood, A. Radiation damage of diamond by electron and gamma irradiation. *Phys. Status Solidi Appl. Res.* **2000**, *181*, 99–107. [[CrossRef](#)]
10. Acosta, V.M.; Bauch, E.; Ledbetter, M.P.; Santori, C.; Fu, K.M.C.; Barclay, P.E.; Beausoleil, R.G.; Linget, H.; Roch, J.F.; Treussart, F.; et al. Diamonds with a high density of nitrogen-vacancy centers for magnetometry applications. *Phys. Rev. B* **2009**, *80*, 115202. [[CrossRef](#)]
11. Schwartz, J.; Michaelides, P.; Weis, C.D.; Schenkel, T. In situ optimization of co-implantation and substrate temperature conditions for nitrogen-vacancy center formation in single-crystal diamonds. *New J. Phys.* **2011**, *13*. [[CrossRef](#)]
12. Botsoa, J.; Sauvage, T.; Adam, M.P.; Desgardin, P.; Leoni, E.; Courtois, B.; Treussart, F.; Barthe, M.F. Optimal conditions for NV-center formation in type-1b diamond studied using photoluminescence and positron annihilation spectroscopies. *Phys. Rev. B* **2011**, *84*, 125209. [[CrossRef](#)]
13. Mindarava, Y.; Blinder, R.; Laube, C.; Knolle, W.; Abel, B.; Jentgens, C.; Isoya, J.; Scheuer, J.; Lang, J.; Schwartz, I.; et al. Efficient conversion of nitrogen to nitrogen-vacancy centers in diamond particles with high-temperature electron irradiation. *Carbon N. Y.* **2020**, *170*, 182–190. [[CrossRef](#)]
14. Mita, Y. Change of absorption spectra in type-1b diamond with heavy neutron irradiation. *Phys. Rev. B* **1996**, *53*, 11360–11364. [[CrossRef](#)] [[PubMed](#)]
15. Collins, A.T. The Fermi level in diamond. *J. Phys. Condens. Matter* **2002**, *14*, 3743–3750. [[CrossRef](#)]
16. Masuyama, Y.; Mizuno, K.; Ozawa, H.; Ishiwata, H.; Hatano, Y.; Ohshima, T.; Iwasaki, T.; Hatano, M. Extending coherence time of macro-scale diamond magnetometer by dynamical decoupling with coplanar waveguide resonator. *Rev. Sci. Instrum.* **2018**, *89*, 125007. [[CrossRef](#)] [[PubMed](#)]
17. Liaugaudas, G.; Davies, G.; Suhling, K.; Khan, R.U.A.; Evans, D.J.F. Luminescence lifetimes of neutral nitrogen-vacancy centres in synthetic diamond containing nitrogen. *J. Phys. Condens. Matter* **2012**, *24*, 435503. [[CrossRef](#)] [[PubMed](#)]
18. Stortebom, J.; Dolan, P.; Castelletto, S.; Li, X.; Gu, M. Lifetime investigation of single nitrogen vacancy centres in nanodiamonds. *Opt. Express* **2015**, *23*, 11327–11333. [[CrossRef](#)]
19. Smith, W.V.; Sorokin, P.P.; Gelles, I.L.; Lasher, G.J. Electron-spin resonance of nitrogen donors in diamond. *Phys. Rev.* **1959**, *115*, 1546–1552. [[CrossRef](#)]
20. Cox, A.; Newton, M.E.; Baker, J.M. ¹³C, ¹⁴N and ¹⁵N ENDOR measurements on the single substitutional nitrogen centre (P1) in diamond. *J. Phys. Condens. Matter* **1994**, *6*, 551–563. [[CrossRef](#)]
21. Manson, N.B.; Harrison, J.P. Photo-ionization of the nitrogen-vacancy center in diamond. *Diam. Relat. Mater.* **2005**, *14*, 1705–1710. [[CrossRef](#)]
22. Shenderova, O.A.; Shames, A.I.; Nunn, N.A.; Torelli, M.D.; Vlasov, I.; Zaitsev, A. Review Article: Synthesis, properties, and applications of fluorescent diamond particles. *J. Vac. Sci. Technol. B* **2019**, *37*, 030802. [[CrossRef](#)]
23. Bauch, E.; Singh, S.; Lee, J.; Hart, C.A.; Schloss, J.M.; Turner, M.J.; Barry, J.F.; Pham, L.M.; Bar-Gill, N.; Yelin, S.F.; et al. Decoherence of ensembles of nitrogen-vacancy centers in diamond. *Phys. Rev. B* **2020**, *102*, 134210. [[CrossRef](#)]

-
24. Davies, G.; Lawson, S.C.; Collins, A.T.; Mainwood, A.; Sharp, S.J. Vacancy-related centers in diamond. *Phys. Rev. B* **1992**, *46*, 13157. [[CrossRef](#)] [[PubMed](#)]
 25. Edmonds, A.M.; D'Haenens-Johansson, U.F.S.; Cruddace, R.J.; Newton, M.E.; Fu, K.M.C.; Santori, C.; Beausoleil, R.G.; Twitchen, D.J.; Markham, M.L. Production of oriented nitrogen-vacancy color centers in synthetic diamond. *Phys. Rev. B* **2012**, *86*, 035201. [[CrossRef](#)]